

iSHM

Structural Health Monitoring



Sensitive. Stable. Autonomous.

PSP Petschacher Software
und Projektentwicklungs GmbH

iSHM: Monitoring Structural Health

Why monitor?

Any large structure is subject to forces that will cause it to deviate from its original design. As a structure ages, components such as bearings will fail, cable stays will weaken and the cumulative effects of cyclic or exceptional loads will reduce the structure's resistance. Over its lifetime the structure must also cope with geological processes, such as settling of the foundations, soil pressure, slippage and erosion. These processes set up a series of forces on the bridge that will cause structural members to bend, change orientation, and shift position relative to one another.

Physical inspections of a bridge will detect these problems before they become a safety issue. However, full inspections are mandated every 6 years and a fault may not be noticed until it is well advanced—and expensive to rectify. Even the most thorough physical inspection only provides a snapshot of a bridge's condition. Transitory or intermittent faults will inevitably be missed; subtle changes that are part of a long-term trend, can all too easily be dismissed as measurement errors. Nor can daily or seasonal patterns be accounted for. Our monitoring systems observe the bridge at hourly or daily intervals. For exceptional events, they can measure at up to 2KHz. Our clients can access up to date bridge data from their own workstation, receive reports (typically every six months) and, if there are

significant changes in the condition of their bridge, they receive an immediate alert.



Ultimately, our systems are designed to help engineers make *informed* decisions. Engineers and bridge managers must decide when maintenance is conducted, whether a bridge's lifetime can be extended or whether a fault will be sufficiently serious to require rectification. All of these decisions are based on predictions of the bridge's future state. The predictions are, in turn, extrapolations from the most recent survey—which may have taken place years before. By measuring the current state of the bridge, our iSHM systems reduce the uncertainty associated with these decisions.

When is iSHM used?

An iSHM system can be used in a number of contexts:

- *Monitoring known faults*—if a non-critical fault has been detected during a physical examination, monitoring its effect on the geometry of the bridge allows an informed decision to be made about the necessity and scheduling of repairs.
- *Bridges nearing the end of their life*—a bridge's design lifetime is a conservative estimate—the majority of bridges are taken out of service prematurely—this has economic and environmental consequences. An SHM system allows engineers to assess the status of a bridge and take corrective actions. With the appropriate information engineers can make decisions about extending the working life of the bridge.
- *Checking healthy bridges*—our systems represent an investment in the future of the bridge. By closely observing the geometry of the bridge, component failures and geological effects are detected early—and can be rectified either during planned maintenance with minimum disruption or with early intervention before the significant damage is inflicted.

The iSHM System

The technical challenge for a bridge logging system is to measure small changes over long periods; and to do so in a harsh physical environment with little infrastructure. PSP systems are a collaboration between experienced electrical and structural engineers—they measure structurally meaningful data in a precise and stable way. Our structural monitoring system has three components, Figure 1,: an

ensemble of sensors tailored to the structure; an on-site logger that interrogates the sensors and a remote server that analyses data and presents results on a web page.

Sensors

The iSHM system is designed to operate with a wide range of sensors, both proprietary and third party; and is compatible with both current loop and Modbus standards. The choice of sensors varies with bridge and application. We offer sensors to measure geometric deviations in the bridge: deflection, displacement and inclination of the structural members. We also have sensors to measure vibration, the internal temperature of the bridge, air temperature and relative humidity. Other sensors are available on request.



Inclination sensor

Lateral displacement sensor
(laser and optical sensor)



Longitudinal displacement sensor
(mechanical)

In most cases, iSHM is used to monitor a previously identified issue, and the system is tailored to address specific areas of concern. Figure 2 shows typical structural issues that may arise for a small bridge, and the sensors used to monitor them.

Figure 1: Overview of iSHM

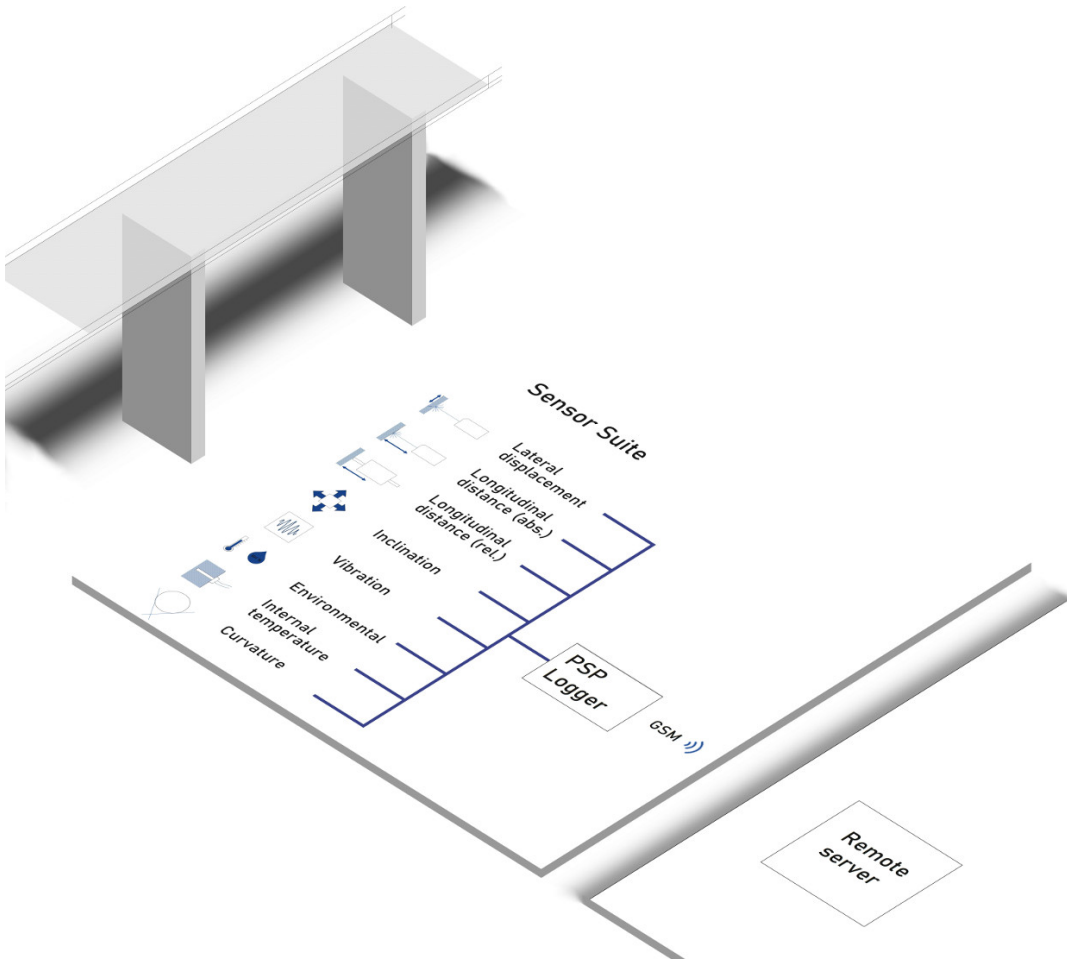
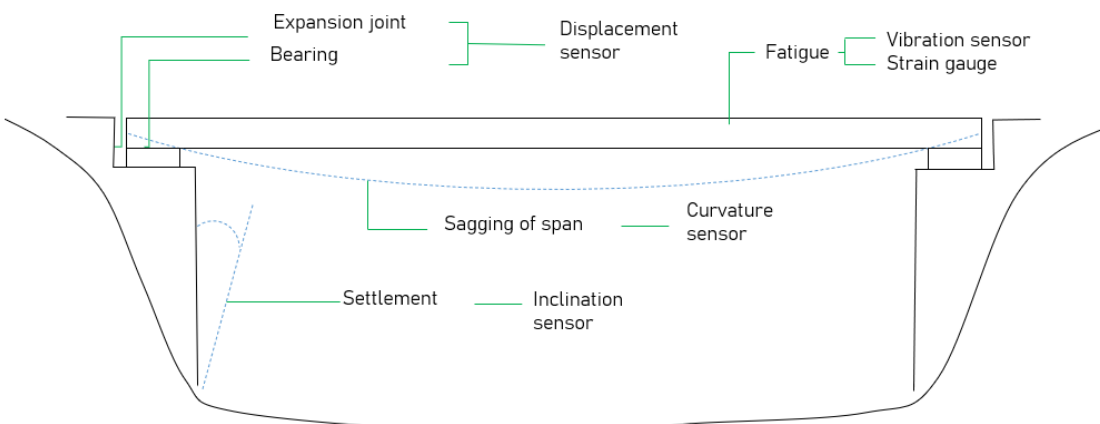


Figure 2: Sensors and their applications



Settlement and other geophysical effects may cause small changes in the orientation of parts of the structure; these can be

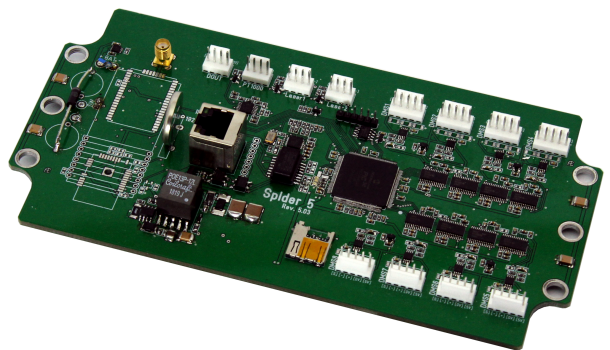
monitored with our inclination sensor. Long term sagging of the span can be measured with our curvature sensor. Issues with bearings and expansion joints can be

monitored with a combination of temperature and displacement sensors. Fatigue can be modelled using data from vibration or strain sensors. iSHMs flexible design and wide range of sensors allows a solution to be tailored to a given task.

Smart Logger

The smart logger can measure up to 8 channels using a high precision 32 bit ADC and has 2 current loop channels. In addition, there is also a bus system than can measure up to 10 nodes. The sampling pattern is programmable: measurements can be taken at intervals ranging from 10s to 24 hours. Detailed snapshots of unusual events can be taken using short bursts of measurements at frequencies of up to 2kHz.

Because the logger must operate from a battery, special attention was paid during design to power consumption. Since the GSM component consumes most power, the logger will cache the measurements on its own removable storage and will only transmit data if it has sufficient reserves in its battery. This means that data transmission will be delayed until the solar cell has been able to charge the battery to the required level. Housed with a steel IP65 case, the logger is robust and reliable. Once installed, the logger typically runs six months without human intervention.



Remote Server

Data received by the remote server is archived, analysed and presented to the user. Data is archived in a secure SQL database. Regression and time series models are used to account for temperature and to resolve meaningful data from background trends, such as daily or season temperature variation. The processed data is presented to users with an easy to use web page, it can also be relayed to the user in Excel files. The remote server is also able to re-configure the logger during the communication window.

PSP provides a range of software tools for the analysis and visualisation of acquired data. Outliers can be detected and suppressed; seasonal and diurnal trends can be modelled and resolved from the measurements. Measurements can be correlated with each other and with temperature to identify relationships. Deviations from these relationships can indicate aberrant behavior of the structure.

Furthermore, high frequency measurements, such as vibration, can also be incorporated into our bridge models. These can be obtained from accelerometers, or they can

be extracted from measurements made by an iBWIM installation. With appropriate signal processing and spectral analysis these measurements can be used to constantly update the lumped parameters of the dynamic model of the bridge. These oscillations can also be used to record the loading cycles of the bridge and so inform the bridge's fatigue model.

The visualisation modules allow the relationships between measurements to be seen more clearly, and unusual behaviour more easily identified. The most obvious example is where we would expect two measurements to follow each other, e.g. the displacement of adjacent bearings, deviations by one of the bearings can be detected, and distinguished from background noise, using classical detection algorithms. These relationships can also be used to make predictions about how the measurement should evolve over time—deviations from the prediction may indicate a fault. The visualisation module also allows physical representations of bridge components to be visualised, either in real-time, or compiled into a time-lapse movie, Figure 4.

Why choose iSHM ?

- Specially designed, proprietary sensors and electronics.
- Flexible: sensor ensemble is tailored for each bridge.
- Self-powered, only requires mobile telephone coverage.
- Sophisticated analysis algorithms, up to date results presented on secure webpage.

How is iSHM used in practice?

Our SHM systems are usually leased for two years. Installation is carried out by PSP and generally takes less than a day. PSP is responsible for maintaining the system. Clients have access to up-to-date data via a password protected webpage. The data can be viewed graphically on the website or the raw data can be downloaded by the clients for their own analysis.

Attached to this document we have included two case studies that illustrate how our systems can be used in practice.



Figure 3: Screenshot: Vibration measurement with iBWIM installation

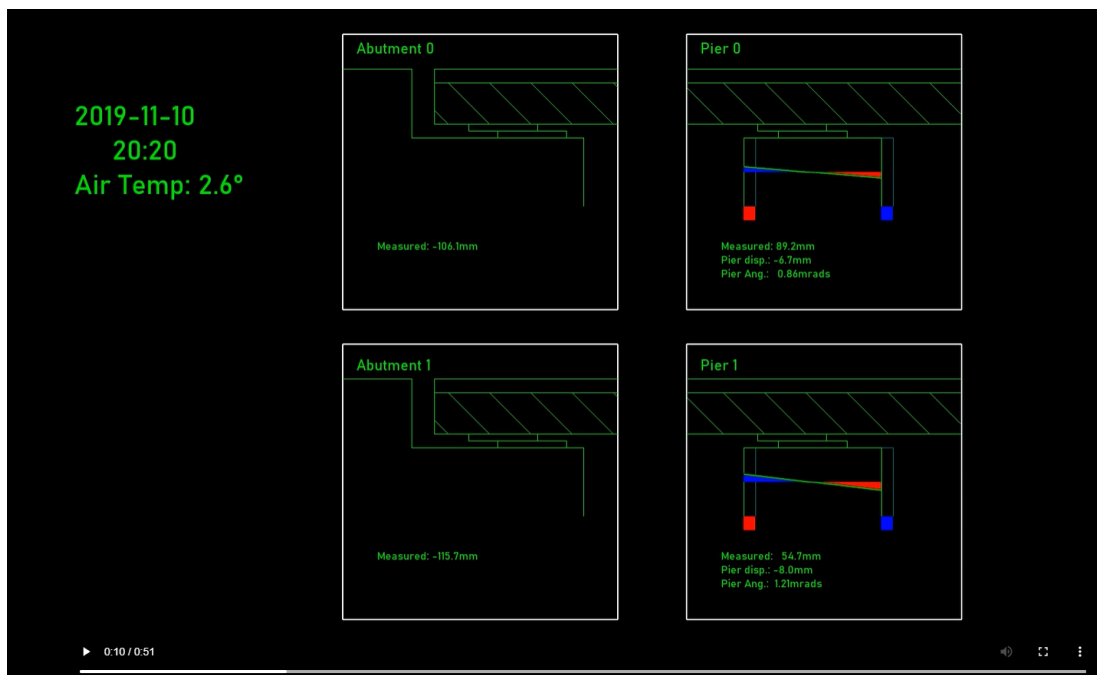


Figure 4: Screenshot: Visualisation of bridge components

For more information contact office@petschacher.at

PSP GmbH Tel. +43 4276 33780
Fax +43 4276 337820 email office@petschacher.at
Am Hügel 4,
A-9560 Feldkirchen
Austria www.petschacher.at

PSP HAS MADE CONSIDERABLE EFFORTS TO ENSURE THE CONTENT OF THIS DOCUMENT IS CORRECT AT TIME OF PUBLICATION BUT MAKES NO WARRANTIES OR REPRESENTATIONS REGARDING THE CONTENT. PSP EXCLUDES LIABILITY, HOWSOEVER ARISING, FOR INACCURACIES IN THIS DOCUMENT.

© 2019 RSR GmbH. All rights reserved.

Case Study 1

Case study 1



Task

Our client owns two adjacent bridges, each is a 4 lane road bridge with a total span of more than 400m and piers arranged in pairs; at their highest points, the bridges are 20m above the valley floor. The bridges were constructed in the 1970's and typically support around 100,000 vehicle journeys daily. During a routine inspection of the bridges in July 2019 a fault was detected in one of the bridge bearings.

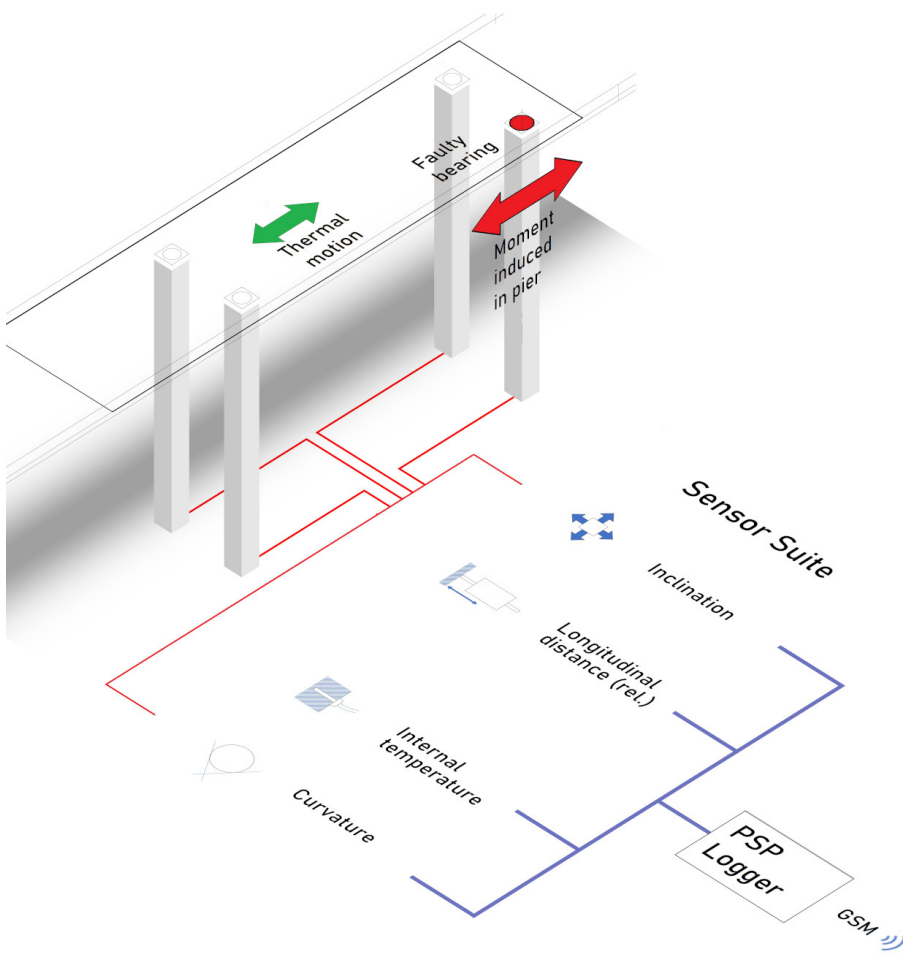
As temperature varies by hour and season, a bridge expands and contracts. The bearings allow the spans of the bridge to move relative to its fixed points. If a bearing resists this motion, the force will be transferred to the pillars of the bridge. This will cause the pillars to buckle and cause expensive structural damage.

Bearings are typically inspected every six years: a fault does not require the immediate closure of the bridge. However, the bearing will need to be replaced; it is only a question of when, and how the repair can be scheduled to minimise disruption. To make this decision, the bridge manager needs to monitor the deterioration of the bearing and its effects on the bridge.

Solution

PSP was asked to provide a monitoring system that could track the severity of the fault and alert the bridge owner if it approached a safety critical level. Our system monitors the curvature and inclination of the piers 24 times a day and reports values back to a remote server. We monitor both piers; measurements from the healthy pier act as reference values. The system was installed in one day with no disruption to traffic. Due to the limited infrastructure on the

bridge, our logger is self-powered and communicates using the mobile phone network. Our logger typically runs for six months without maintenance. Analysis of the inclination and curvature of the piers takes place on a remote server. Data is made immediately available to the client via a secure webpage. Reports on the bridge status are prepared every six months. We categorise the bridge status as red, green or amber. Significant changes in the status of the bridge trigger an immediate physical examination of the bridge.



We placed instruments on four piers: the pier with the faulty bearing, the adjacent pier and two nearby but unaffected piers. Displacement sensors, to monitor the relative position of the pier to the bridge superstructure, were placed on all four piers. Inclination sensors to monitor the orientation of the piers, and curvature sensors to monitor their bending, were placed on the two affected piers. Sensors to measure the internal temperature of the bridge were placed on either side of the bridge.

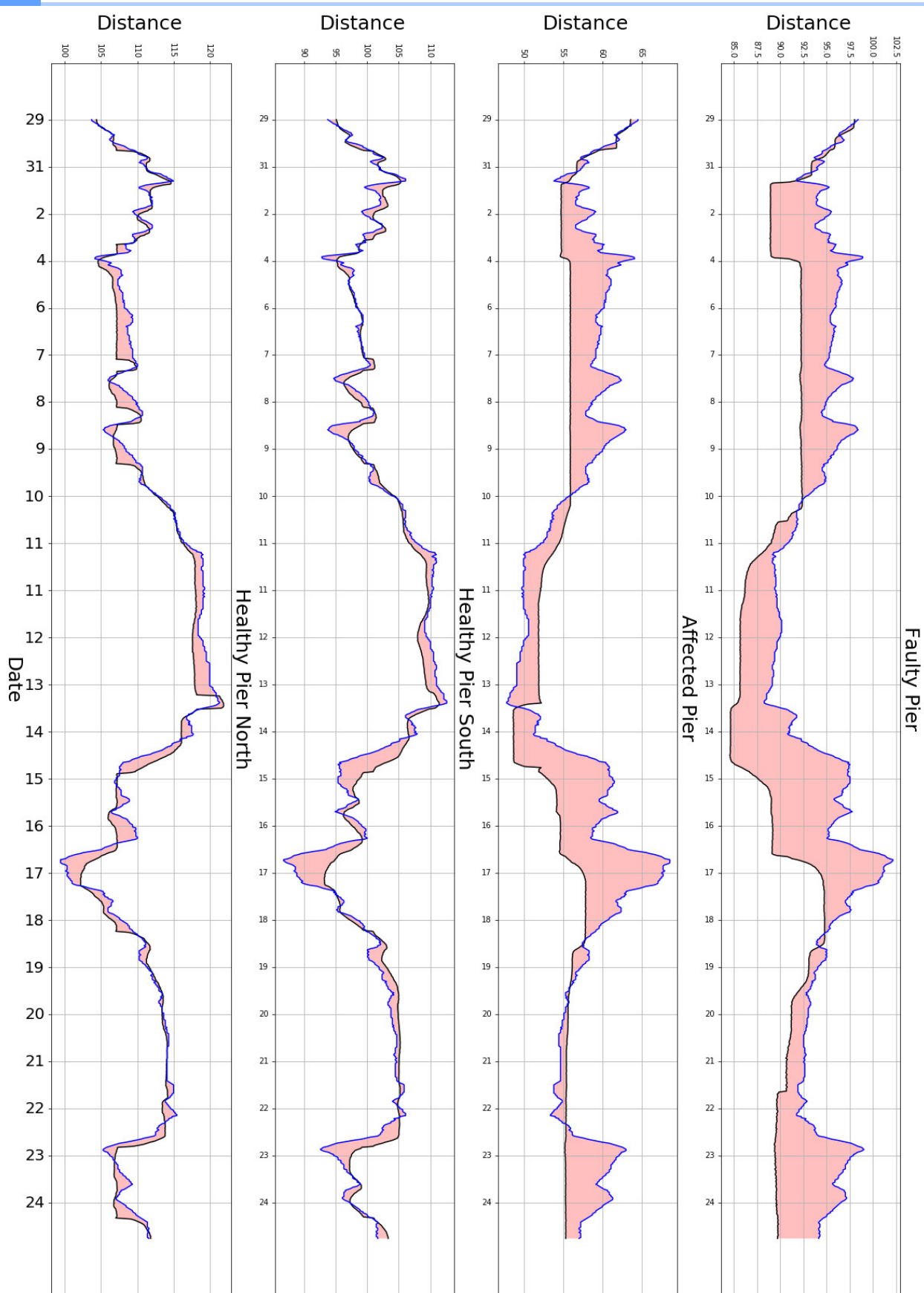
If we treat the bridge as a system, then the driving function is the internal temperature of the

bridge. Temperature drives the expansion and contraction of the bridge, and when that motion is resisted, it deforms the bridge. The bridge's temperature depends on the ambient temperature and on direct sunlight. Our client's bridge runs from east to west; the south side of the bridge is exposed to more direct sunlight and is significantly warmer than the north. Since expansion varies linearly with temperature, if the bearing is functioning, the relative displacement between the bridge and the pier will follow the same curve as temperature. If the bearing should fail, and the bridge and pier become locked together, there will be a discrepancy between our prediction and our measurement of position. The discrepancy between where the bridge should be, and where it actually is, is taken up by the distortion of the pier.

Results

We plot the distances between the bridge superstructure and the pier at the bearings on the graph below. If the bearings are functioning correctly the displacement should track our temperature based prediction. However in the curves for the fault pier and the affected pier there are several plateaus, i.e. the bearing is sticking and the displacement is not changing. We can quantify the effect by measuring the difference between our measurement of the bridge's position and our prediction, coloured in pink. The discrepancy between the thermal prediction and the measurement, represents the distance the bridge must accommodate by deformation. The healthy piers match the prediction well, however there are large discrepancies in the fault and affected piers. Should these discrepancies exceed pre-defined limits the responsible authorities will be alerted.

The PSPLogger costs approximately 0.1% of the value of the bridge and was quickly installed without disrupting traffic. By monitoring the bridge's behaviour closely, bridge planners were able to confidently postpone replacement of the bearing to coincide with scheduled renovation work. This meant the replacement could be carried out more cheaply and with less disruption to traffic.



Case Study 2

Case study

Our client commissioned PEC ZT-GmbH to undertake an analysis of the vibrations present on the test bridge. The analysis has two parts: first a numerical model of the bridge is constructed and used to predict the characteristic frequencies of the bridge; second, vibration measurements of the bridge under normal traffic loading were made and compared with the predictions to verify the model.

The bridge consists of four spans, one of which crosses the river, our investigation is limited to this span. This span is a steel arch bridge 81m long and 15.3m wide. The measurements were performed on the afternoon of 04/03/2021. Two sensors were placed 20m on either side of the bridge centre. Measurements were made on the north side of the bridge.



Figure 1: Measurements in progress.

We measure four classes of vibration. First, a simple deformation along the longitudinal axis of the bridge with nodes at the bearings and an anti-node in the centre of the span., Figure 2, left. The second class is also longitudinal, however this class has an additional node in the centre of the bridge and anti-nodes at the quarter and three quarter points, Figure 2, right. Because the bridge will generally be loaded asymmetrically along the transverse direction, we also measure torsional vibration modes, Figure 3. As with the longitudinal modes, we measure both the one and two (corkscrew) anti-mode cases (along the longitudinal axis).

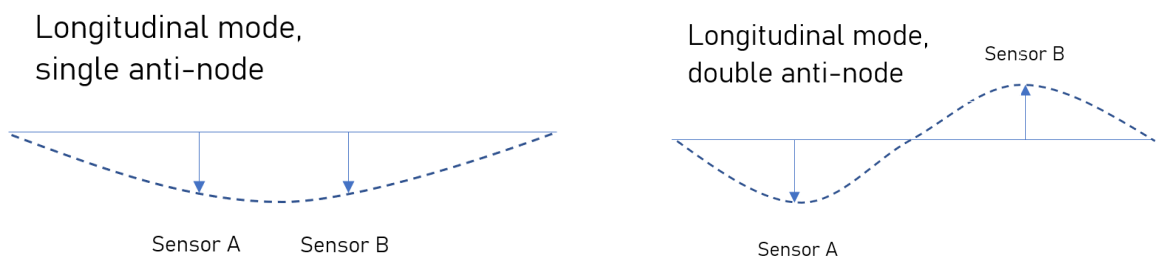


Figure 2: Vibrational modes, longitudinal axis.

In addition to measurements, we undertook Finite Element simulations to predict the vibrations

present on the bridge. The simulation and measurements are used to confirm and support each other. By comparing the measured and predicted resonant frequencies, it is possible to optimise the parameters of the simulation model — improving the quality of the model for other tasks. The four bending modes, and their predicted frequencies are shown below.

This report focuses on two topics: the spectral properties of the signals and the symmetry of the sensors. An initial inspection and description of the signals lets us decide on an approach to the subsequent analysis. Spectral analysis: the spectral properties of the vibration signals can be compared with the predictions of our simulation models. This allows us to verify and improve our bridge model. Symmetry: the relationship between the signals from the two sensors tells us about the relative motion of the bridge: are different parts of the bridge moving in phase with one another, or are they moving in different directions. However, we begin with an initial inspection and description of the signal that will guide the subsequent analysis.

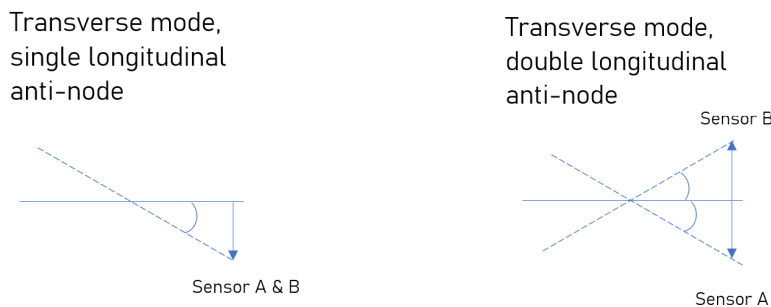


Figure 3: Vibrational modes, transverse axis.

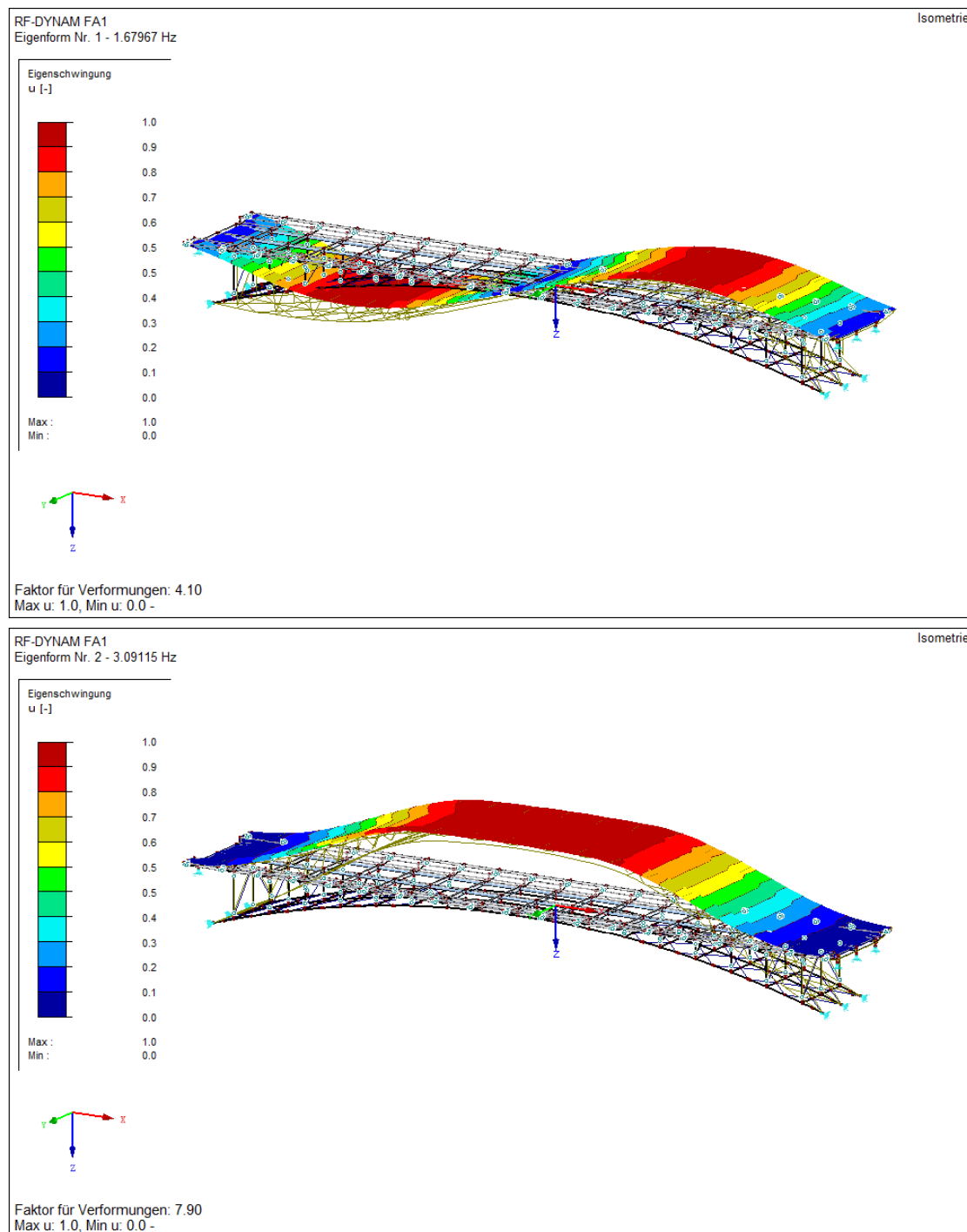


Figure 4: Vibrational modes, longitudinal.

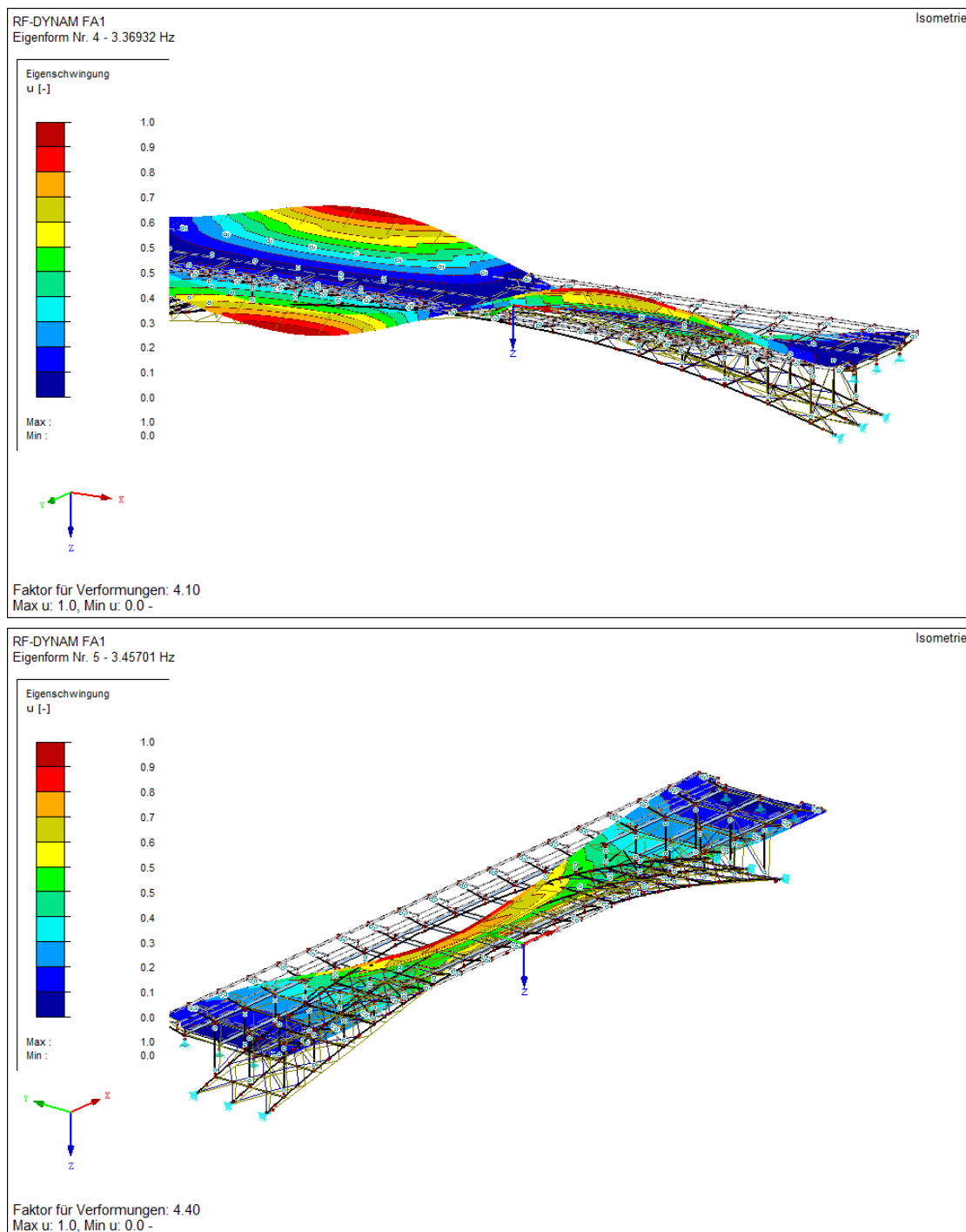


Figure 5: Vibrational modes, transverse.

Analysis

The sensors each measure acceleration in three orthogonal directions: X accelerations along the longitudinal axis of the bridge; Y accelerations along the transverse axis; and Z accelerations in the vertical direction. The Z measurements are the most important, the Y measurements are affected by torsional vibrations; the vibrations measured in the X axis are small and are linked to the longitudinal vibrations.

The sensors report acceleration scaled by the gravitational field, i.e. in g's. The sensors can measure in the range $\pm 2.0g$ with an accuracy of $\pm 0.02g$. Due to the earth's gravitational field, measurements in the Z axis are offset by a value of $1g$ (9.81 ms^{-2}). Values reported in this report are converted to mm s^{-2} and the gravitational offset has been subtracted. The measurements were sampled at 500Hz in short bursts of between 10 to 20 seconds.

Acceleration signal description

The standard deviation of the signal corresponds to its magnitude. Comparison between the axes, Table 1, shows that the Z axis dominates.

TABLE 1: Standard deviation of measurement signals.

Axis	Sensor A	Sensor B
	mms^{-2}	mms^{-2}
X	0.61	0.56
Y	1.25	1.19
Z	2.54	2.19

A typical signal from sensor A along the Z axis of duration 10 seconds is shown in Figure 6. By inspection we can see a high frequency component that is present over most of the record that is three or four short bursts or events, which exhibit a longer periodicity. We can observe the high frequency component more easily if we consider a short section (1s) of the record, Figure 7.

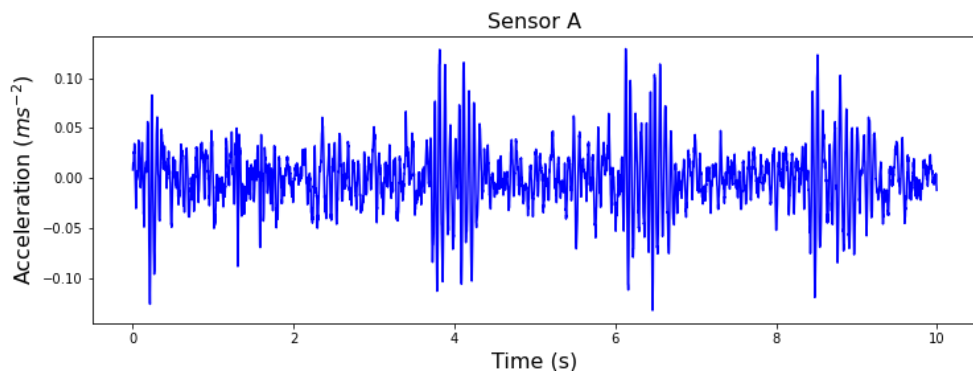


Figure 6: Typical signal from Sensor A

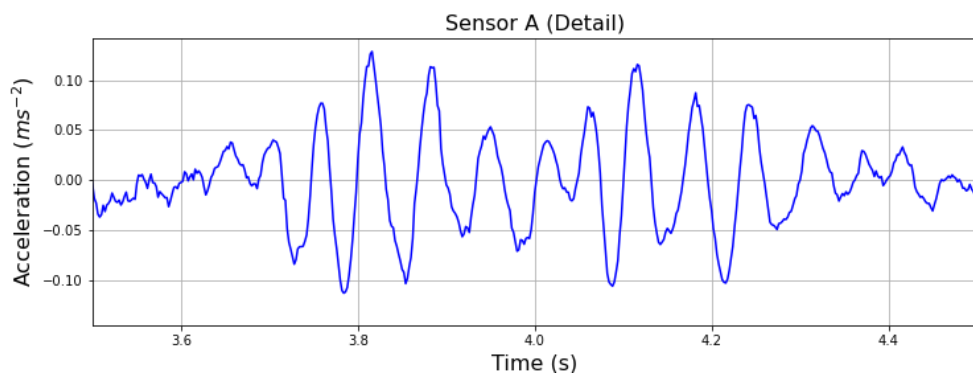


Figure 7: Detail of signal (1 second duration) showing high frequency components.

Power Spectra

We have observed that the signal exhibits characteristic behaviours in different frequency ranges. We now analyse the spectra of the vibration signals. We took record lengths of 10 seconds, giving a nominal frequency resolution of 0.1Hz. Signals less than 10 seconds were discarded; for signals between 10 and 15 seconds a single record was extracted, and for longer signals, multiple overlapping records were extracted and processed with a periodogram. The records were windowed with a Gaussian window with standard deviation of 1.5 seconds. The spectra from all the records from a given sensor were then averaged. The spectra follow the form shown in Figure 8 left .

The measured spectra confirm our earlier observation that the signal has a low frequency and high frequency component. The low frequency component (less than 6Hz) consists of narrow spectral peaks that correspond to structural vibrations in the bridge. The high frequency components are more broadband in nature and correspond to local deck vibrations—these are irrelevant to our analysis. Furthermore, since displacement can be calculated from acceleration using a double integration—equivalent to scaling the PSD by a f^{-4} factor, high frequencies are almost irrelevant to the actual displacement of the sensor locations. We can effectively suppress the high frequency components with a low pass filter Figure 8 (right). Where we calculate values from the signal we will use the low pass filtered signal.

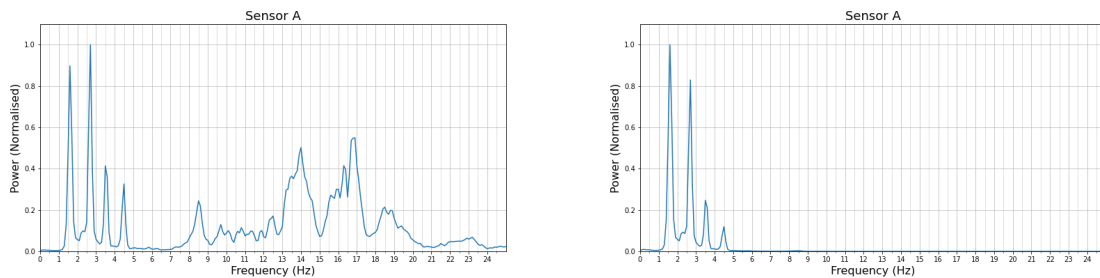


Figure 8: Power spectral density of Z signals from Sensor A (left) and low pass version (right).

Comparison of the standard deviations between the low pass filtered axes, Table 2 shows that the Z axis dominates. In terms of signal energy, the Y-axis signal has approximately 10% and the X axis signal having less than 3% of the Z axis signal energy.

Table 2: Standard deviation of low pass filtered measurement signals.

Axis	Sensor A	Sensor B
X	mm/s ²	mm/s ²
Y	0.15	0.14
Z	0.30	0.31
	0.91	0.91

The greatest challenge for analysis of these signals is their short duration relative to their

wavelength. This limits our ability to distinguish neighbouring frequencies. Furthermore, this is a physical upper bound—analogous to the Uncertainty Principle, and exists irrespective of the type of equipment or processing. As already noted, the record length gives an upper bound of 0.1Hz for resolution; this is further reduced by the required windowing. However, we can achieve a higher resolution by fitting Gaussians to the calculated PSD and interpolating the peak centres Figure 9. That is, we are able to achieve superresolution by assuming that the peaks follow Gaussian distributions. This assumption is partially justified by our use of a Gaussian windowing function. Where we specify numerical values for characteristic frequencies, they are calculated in this way. Using the assumption of a Gaussian distribution to infer frequencies more accurately.

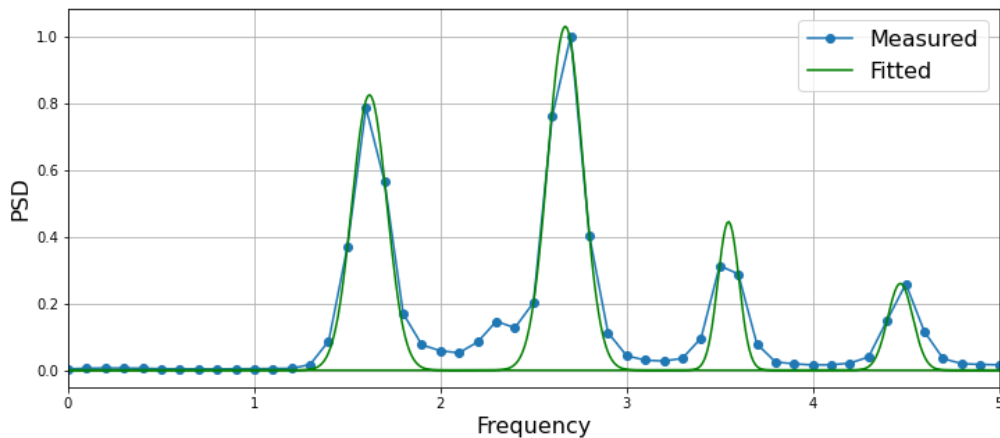


Figure 9: Fitting Gaussians to PSD

The power spectra of signals from sensor A are shown in Figure 10, and those from Sensor B in Figure 11. Comparing the signals from each sensor, axis by axis, we can see that while the amplitude of the peaks varies, their location does not. The locations of the peaks are shown in Table \ref{tab:peakLoca}. The X and Z signals share every component except 2.2 Hz; the Y signals consist of only two components (2.2 and 2.7Hz) both shared by the Z signal. It seems likely then that the 2.2Hz and 2.7Hz components relate to torsional modes.

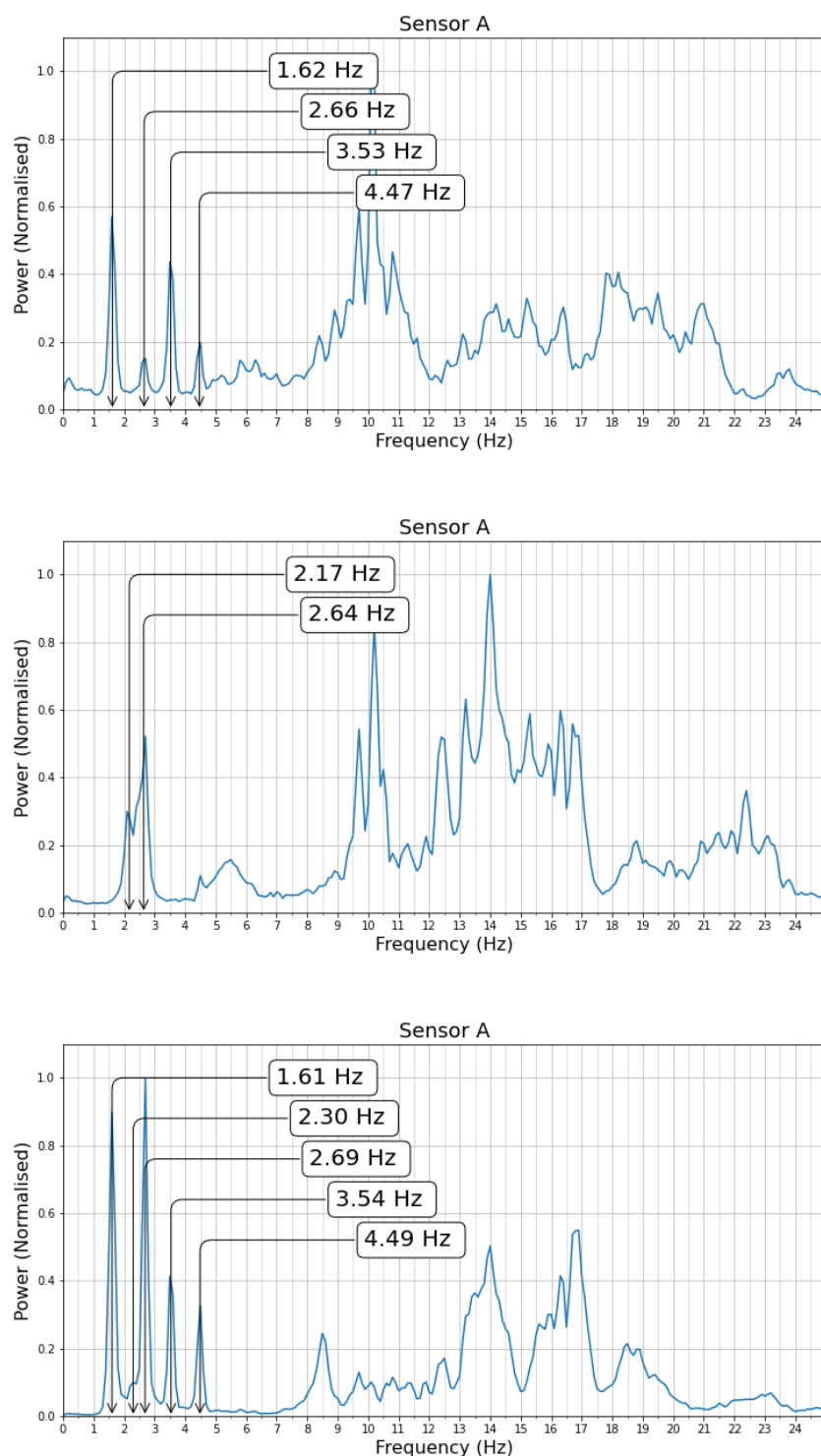


Figure 10: Power spectral density of X,Y and Z signals from Sensor A.

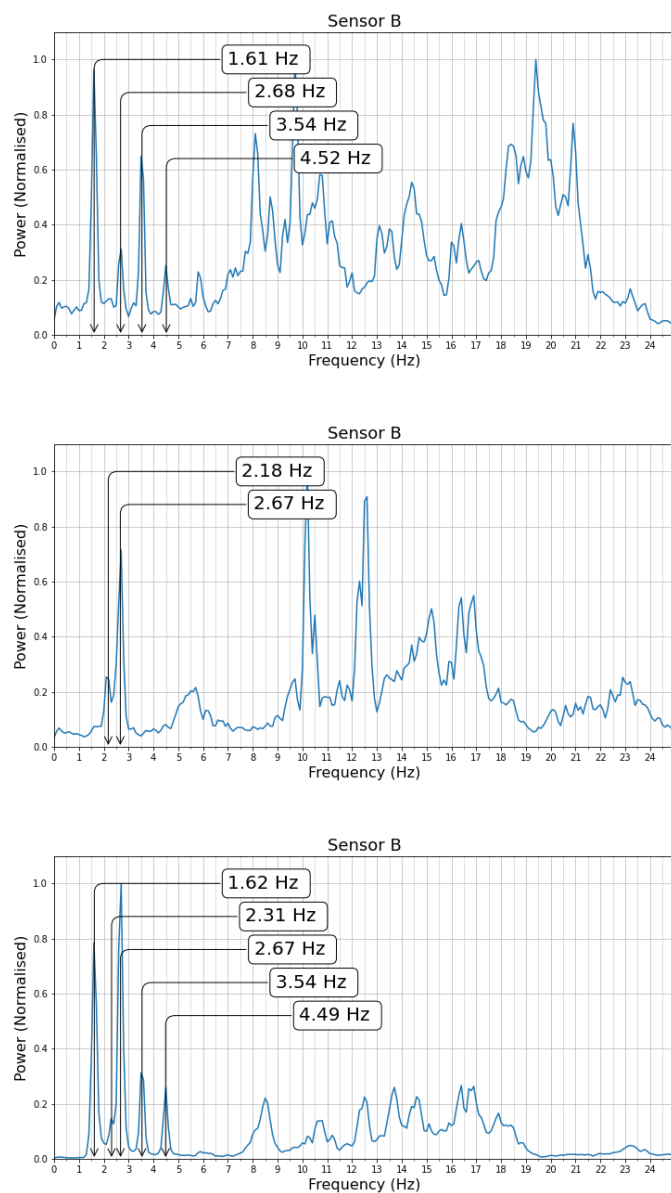


Figure 11: Power spectral density of X,Y and Z signals from Sensor B.

Table 3: Low frequency components in measured signals.

X (Hz)	Y (Hz)	Z (Hz)
1.6		1.6
	2.2	2.3
2.7	2.7	2.7
3.5		3.5
4.5		4.5

Balance

If we compare the signals from the two sensors we can see definite similarities—even in the unprocessed signals. In some cases the signals appear to be in phase, or other cases they seem to be 180° out of phase. This is important for our understanding of how the bridge vibrates: if there is a node near the centre of the bridge we would expect the acceleration signals to be equal and opposite; if there is an anti-node at the bridge centre we would expect sensors to agree in both magnitude and direction.

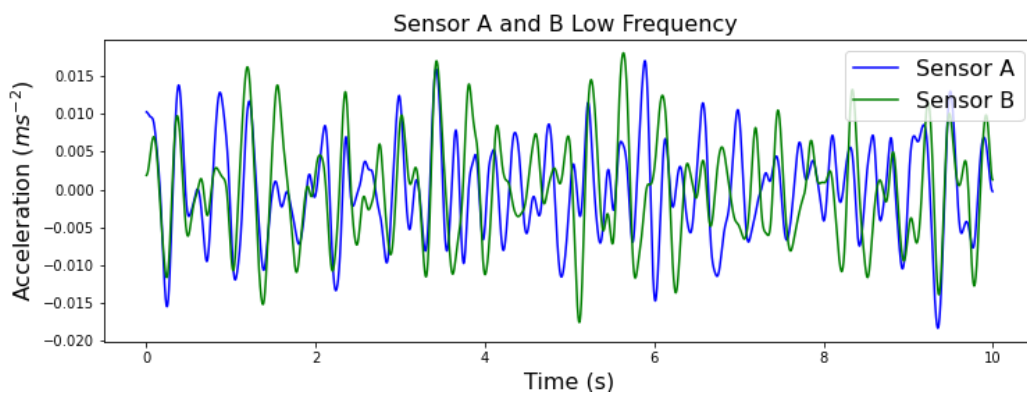


Figure 12: Detail of signals from sensors A and B.

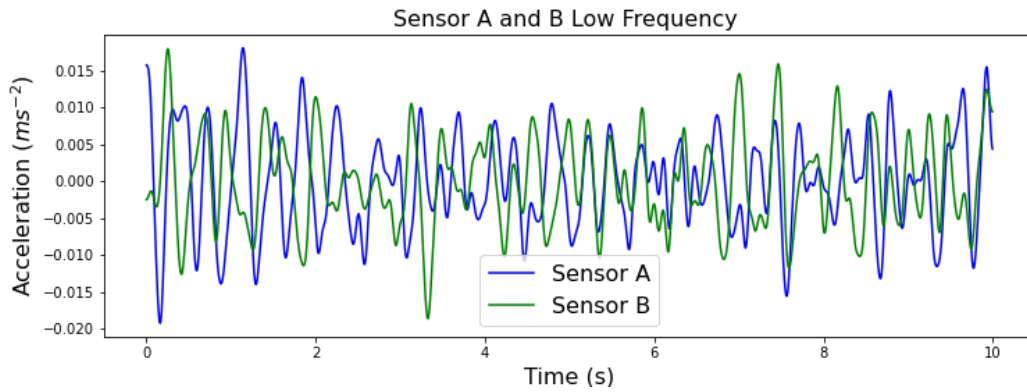


Figure 13: Detail of signals from sensors A and B from another record. If we add the signals from each sensor we generally get a sinusoid with a similar magnitude to the original signals, Figures 15 and 16. We can quantify this effect using the metric $\$b\$$ shown below for each sensor pair. When the signals are 180° out of phase the metric will approach 0; when the signals are in phase the metric will approach unity.

We will now compare the signals mode by mode. That is, for each eigenfrequency we will filter both sensor A and B with a narrow band filter centered at that frequency. We will then calculate the balance metric for the filtered signals, Table 4. The Z signals show strong evidence for single anti-node behaviour at 2.2, 3.5 and 4.5Hz. The vibration mode at 1.6Hz appears to have a node in the centre of the bridge. For the 2.7Hz vibration the balance metric is intermediate. The metric for Y axis vibration at 2.2Hz approaches one, suggesting a maxima at the (longitudinal) centre of the bridge. At 2.7Hz, the metric is intermediate for the Y-axis. In the case of the X-axis,

in contrast to the Z-axis, we get a strong indication at 1.6Hz that the sensors are moving in synchronisation, with the other frequencies being indeterminate.

Table 4: Balance metric in low frequency components.

Frequency	X	Y	Z
1.6	0.93	0.17	
2.2		0.91	0.87
2.7	0.66	0.49	0.62
3.5	0.34		0.97
4.5	0.5		0.99

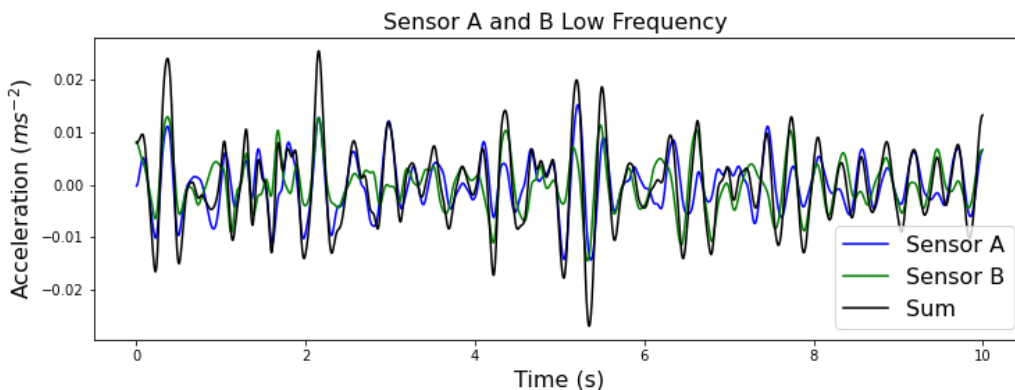


Figure 15: Low frequency components and their sum.

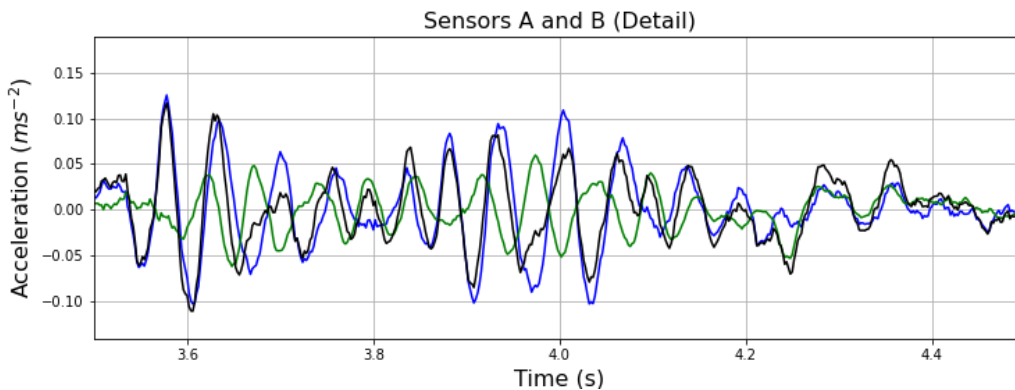


Figure 16: High frequency components and their sum.

Conclusions

This report focused on two topics: the spectral properties of the signals and the symmetry of the sensors. Spectral analysis: Examination of the power spectra showed multiple narrowband peaks below 6Hz as predicted by our simulations. For vertical vibration we found peaks at 1.6Hz, 2.2Hz, 2.7Hz, 3.5Hz and 4.5Hz. Lateral vibration showed peaks at 2.2 and 2.7Hz, indicating torsional vibration modes.

Sensor symmetry: The signals from sensors A and B show many structural similarities. Their relative magnitudes and directions give us an insight into the relative motion of different parts of the bridge. In fact the signals exhibit a variety of behaviors, sometimes in phase, other times in anti-phase. In the case of vertical vibration modes, we found that the 2.2Hz, 3.5Hz and 4.5 Hz modes showed strong symmetry, i.e. the sensors were being accelerated in the same direction at the same time. At 1.6Hz, we found that the sensors were being accelerated in opposite directions at any given time. In the case of lateral (Y) vibration at 2.2Hz, we found that this mode caused the sensors to accelerate in the same direction.

Feldkirchen, March 11, 2021